Available online at www.sciencedirect.com
SCIENCE DIRECT®
PERGAMON
Chaos, Solitons and Fractals 18 (2003) 385–399
CHAOS SOLITONS & FRACTALS
www.elsevier.com/locate/chaos

Monofractal and multifractal characterization of geoelectrical signals measured in southern Italy

Luciano Telesca [a,*], Gerardo Colangelo [a], Vincenzo Lapenna [a], Maria Macchiato [b]

[a] *Institute of Methodologies for Environmental Analysis, National Research Council, Tito Scalo (PZ) 85050, Italy*
[b] *Dipartimento di Scienze Fisiche, Università "Federico II", Naples 80125, Italy*

Abstract

Fractal tools have been used to characterize the temporal fluctuations in the dynamics of hourly geoelectrical signals, measured from January 2001 to February 2002 by four stations installed in Basilicata region (southern Italy). Three stations (Giuliano, Marsico and Tito) are located in a seismic area, and one (Laterza) in an aseismic area. Monofractal approaches (Lomb Periodogram, Higuchi method and detrended fluctuation analysis) have been used to identify in a wide range of timescales scaling behaviour, that indicates the presence of correlated temporal fluctuations and long-range dependence. The multifractal formalism leads to the identification of a set of parameters, derived from the shape of the multifractal spectrum (the maximum α_0, the asymmetry B and the width W) and measuring the "complexity" of the signals. Furthermore, the multifractal parameters have revealed to well discriminate geoelectrical signals measured in seismic areas from those recorded in aseismic areas.

1. Introduction

The investigation of the temporal fluctuations in self-potential signals could provide indirect information on the dynamics underlying the tectonic processes. Geoelectrical parameters may be useful to monitor and understand many seemingly complex phenomena linked to seismic activity [1,2]. Variations in the stress and fluid flow fields can produce changes in the self-potential field, in resistivity, and in other electrical parameters [3], so that investigating these induced fluctuations may give information on the governing mechanisms both in normal conditions and during intense seismic activity.

During the last decades many anomalous spatial and temporal patterns in electrical signals have been observed, possibly linked to incoming earthquakes, or correlated with seismic activity [4,5]. Successes and failures in the earthquake prediction have been analyzed; however, a firm quantitative methodology, based on an effective knowledge of the time dynamics of the electrical signals, is needed to select anomalous patterns from the background noise. In this way it is a very hard task to obtain a complete and robust statistical evaluation of the efficiency of the electrical precursors [6,7].

For this reason, the use of electrical precursors in earthquake prediction is to a large extent still empirical, due to the many difficulties that still exist in understanding the physics underlying the source mechanisms of geophysical precursory phenomena [3], and to the well-defined objective criteria to evaluate the reliability of the short-term predictions based on this type of precursory signals.

* Corresponding author. Tel.: +39-971-427-206; fax: +39-971-427-271.
E-mail address: ltelesca@imaa.cnr.it (L. Telesca).

0960-0779/03/$ - see front matter
doi:10.1016/S0960-0779(02)00655-0

In order to assess the use of geoelectrical signals as indicators of earthquake preparation [8,9], the fundamental issue to address is if these parameters are able to reveal dynamical characteristics of active tectonics. Obviously, the existence of such a correlation can be established only after a dynamical characterization of the geoelectrical signals is performed. In the framework of this strategy, we investigate in this work the dynamical properties of geoelectrical signals, as they can be detected from observational time series. In order to reach this goal we used several fractal and multifractal methods to analyze the structure of the temporal fluctuations in geoelectrical data.

In a previous paper Cuomo et al. [10] analyzed the geoelectrical daily means in order to give information about the statistical features of the geoelectrical background noise and the inner dynamics of geophysical processes producing the electrical phenomena observed on earth surface in seismic areas. They discussed the statistical analysis of dynamical systems based on the estimation of their degree of predictability, distinguishing randomness from chaos and providing a parsimonious representation in terms of autoregressive models of observations, by means of the only information coming from the time series itself.

Geoelectrical signals are the result of the interaction among very heterogeneous and not well known mechanisms. In particular, there are many ambiguities to indicate a common physical process able to describe the possible generation of electrical signals in seismic active areas. A reasonable common physical process could be the dilatancy-diffusion-polarization model [11]. Local features can be mixed with the general ones [12] so increasing the difficulty of rightly characterizing and interpreting the signal time variations.

In the study of seemingly complex phenomena, like those generating geoelectrical signals, methodologies able to determine time scale structures in observational time series are particularly useful tools to obtain information on the features and on the causes of variation at the different time scales. In particular fractal analysis methods, developed to extract quantitative and qualitative information from time series, have recently been applied to study a large variety of irregular signals and to detect deep dynamical features.

In this paper we apply monofractal and multifractal methods in order to characterize the temporal fluctuations of the geoelectrical time series.

2. Geological and seismological settings

The measuring stations are located on the Southern Apennine chain which consists of a pile of thrust sheet forming a complex system orogenically transported over the flexured South-Western margin of the Apulia foreland. Quaternary volcanitic rocks of the Mt.Vulture volcanic complex separate the Apulia platform from the Campania–Basilicata segment. An extensive distribution of intrasedimentary tertiary and quaternary volcanic bodies at depths ranging from 9.5 to 12 km are also recognizable [13]. The Southern Apennine chain is one of the most active area of the Mediterranean region. It is the result of a complex sequence of tectonic events associated with the collision between Africa and Europe.

The South Apenninic fault structure and the connected complex rupture events of the surface are strictly linked with deep originated fluid occurrences, such as geothermal manifestations, mofettes, etc. strongly affected by preseismic phenomena reported in the historical and recent seismicity phenomena [11,14,15]; so it is possible to detect electrical anomalies possibly related to electrokinetic phenomena. Obviously we cannot exclude the presence of other generation mechanisms of electrical phenomena, because up to now a complete theory about this topic is not available.

Therefore, taking into account the seismological and the peculiar geological settings, we selected this area to install the geoelectrical monitoring network, constituted by four stations (Fig. 1). Each station measures one to four self-potential signals. The hourly self-potential data, recorded during the period January 2001–February 2002, are plotted in Fig. 2. From a visual inspection, the time series show erratic fluctuations, that could exhibit unexpected hidden scaling structure. The number of hourly data record is sufficient to perform the analyses with reliable estimates of the exponents.

3. Methods

3.1. Monofractal methods

To quantitatively characterize geoelectrical signals, we need to use techniques able to extract robust features hidden in these complex fluctuations.

Various methods for analyzing the correlation properties of a time series are available, and many techniques have been developed to detect and quantify fractal features in experimental and observational data.

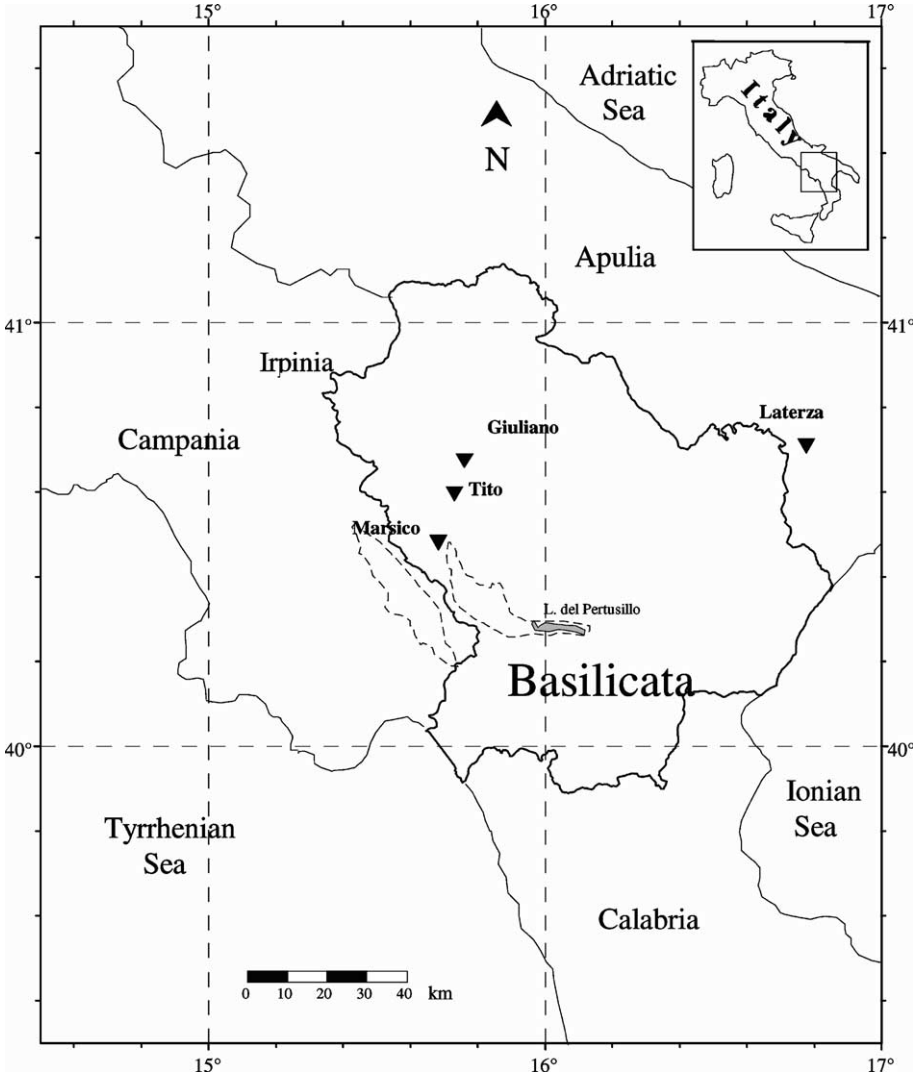

Fig. 1. Ubication of the geoelectrical monitoring network in southern Italy.

The spectral analysis represents the standard method to evaluate the presence of purely random fluctuations in time series. Signals, whose samples are uncorrelated among them, are characterized by a flat power spectrum (white noise); while signals, whose samples are long-range correlated, are characterized by a power spectrum decreasing with the frequency, $S(f) \propto f^{-\beta}$, where β indicates the degree of correlation (coloured noise). For unevenly sampled time series the power spectrum can be calculated by means of the Lomb Periodogram method [16]. Denoting as x_n the datum measured at instant t_n, the Lomb Periodogram is defined by the following formula:

$$P(\omega) = \frac{1}{2\sigma^2}\left\{\frac{\left[\sum_n (x_n - \bar{x})\sin\omega(t_n - \tau)\right]^2}{\sum_n \sin^2\omega(t_n - \tau)} + \frac{\left[\sum_n (x_n - \bar{x})\cos\omega(t_n - \tau)\right]^2}{\sum_n \cos^2\omega(t_n - \tau)}\right\}, \tag{1}$$

where $\omega = 2\pi f$ is the angular frequency and τ is given by

$$\tan(2\omega\tau) = \frac{\sum_n \sin 2\omega t_n}{\sum_n \cos 2\omega t_n}. \tag{2}$$

The slope of the line fitting the log–log plot of the power spectrum by a least square method in the linear frequency range gives the estimate of the spectral index β.

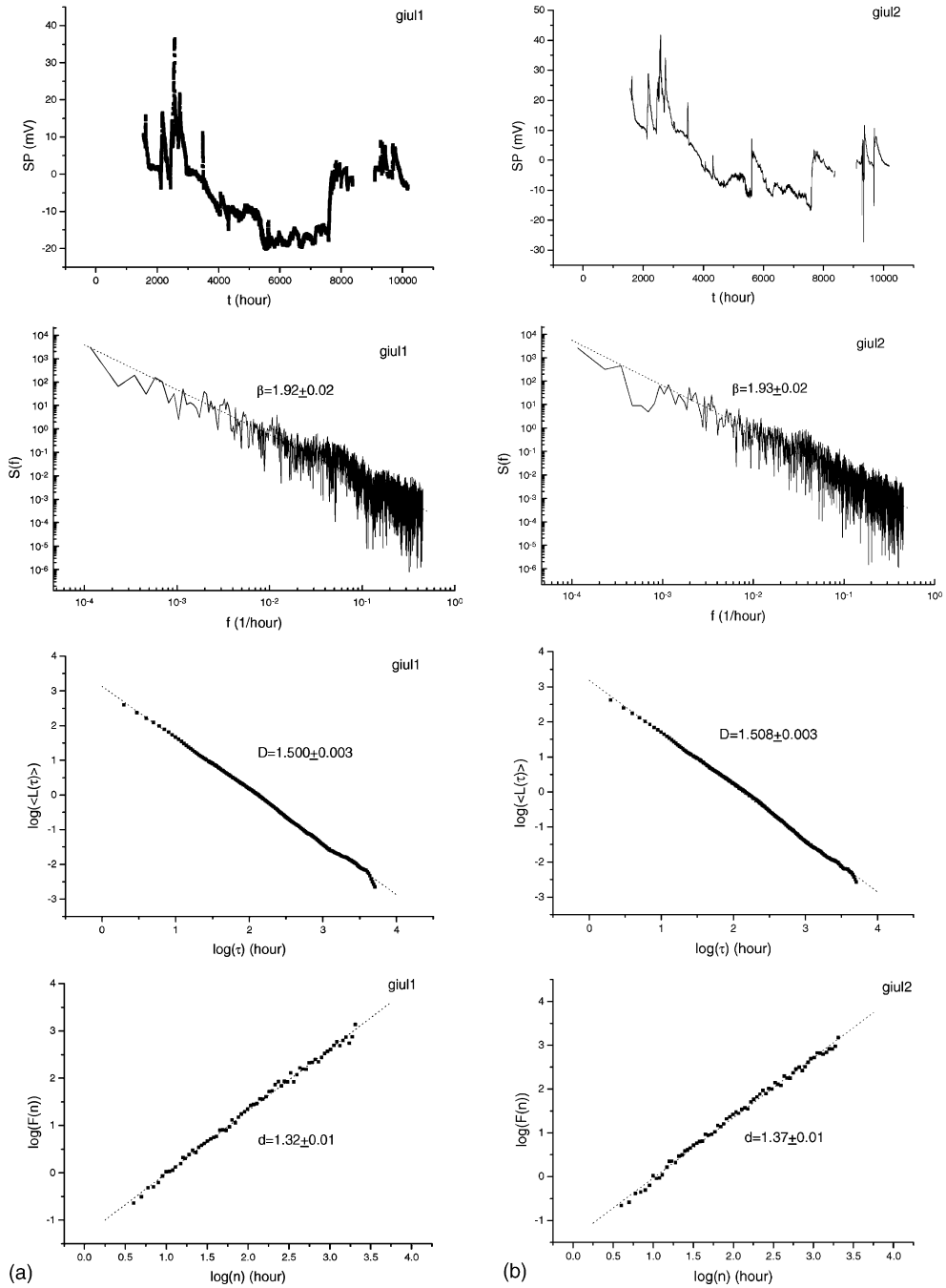

Fig. 2. Hourly variability, Lomb spectra, Higuchi analysis and DFA of the nine geoelectrical signals recorded at stations (Giuliano, Marsico, Laterza and Tito), located in southern Italy. All the statistics performed reveal the presence of correlated structures in the data, indicating the presence of memory effects in the geophysical systems governing the time dynamics of the signals.

A more stable estimate of the spectral exponent can be performed by the calculation of the fractal dimension of the signal using the Higuchi method [17,18]. In the literature, many papers have been devoted to find methods capable of giving stable estimations of the power-law spectral index. Burlaga and Klein [19] presented a method to calculate stable values of the fractal dimension D of large-scale fluctuations of the interplanetary magnetic field; the relationship

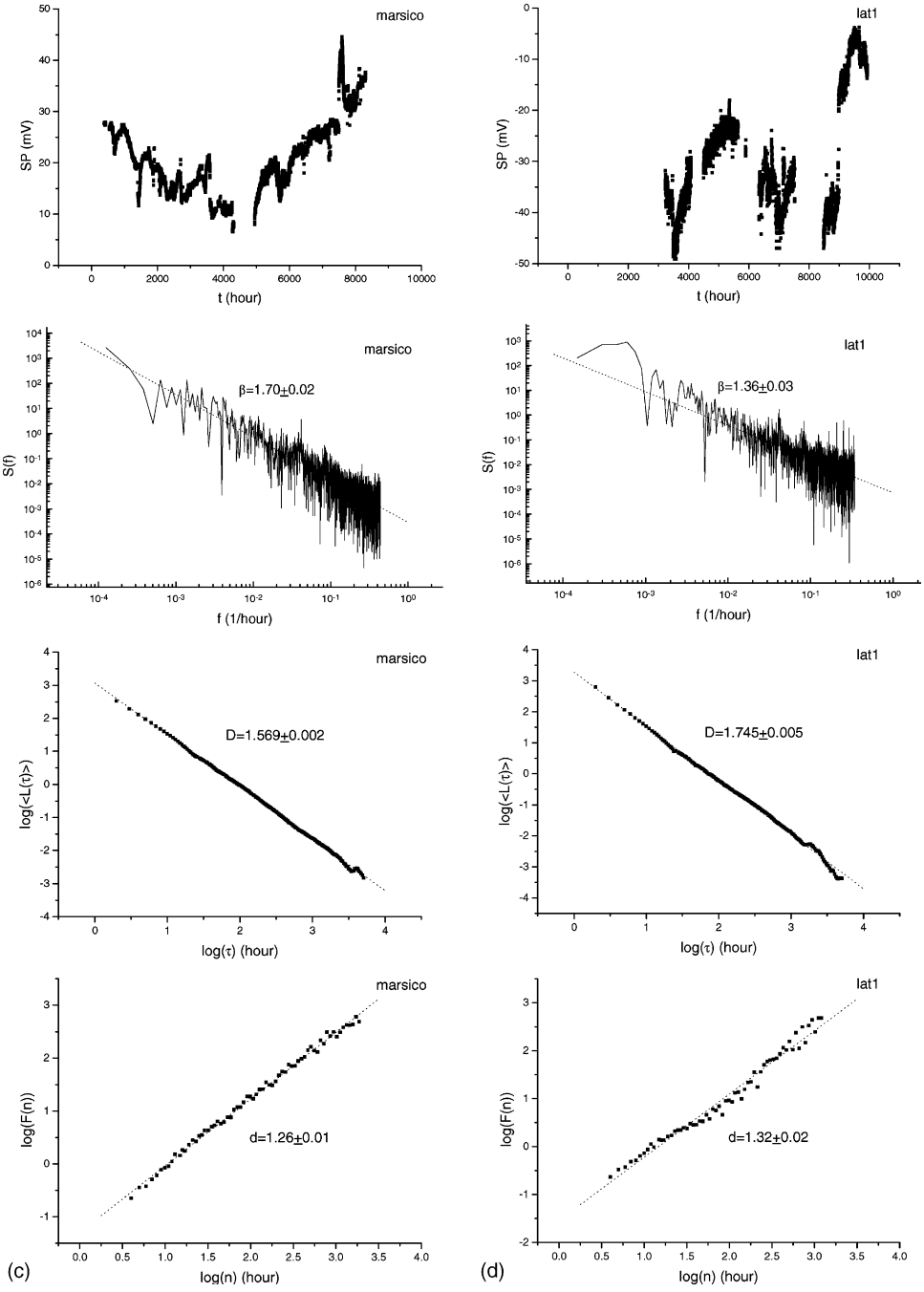

Fig. 2 (*continued*)

between the fractal dimension D and the spectral exponent β is given by Berry's expression $D = (5 - \beta)/2$ [20], for $1 < \beta < 3$. They defined the length $L_{BK}(\tau)$ of the $B(t)$ curve as

$$L_{BK}(\tau) = \sum_{k=1}^{N} |\bar{B}(t_k + \tau) - \overline{B}(t_k)|/\tau, \tag{3}$$

where $\overline{B}(t_k)$ denotes the average value of $B(t)$ between $t = t_k$ and $t = t_k + \tau$. This length is a function of τ, and for statistically self-affine curves, the length is expressed as $L_{BK}(\tau) \propto \tau^{-D}$. Using this relation, the value of D can be

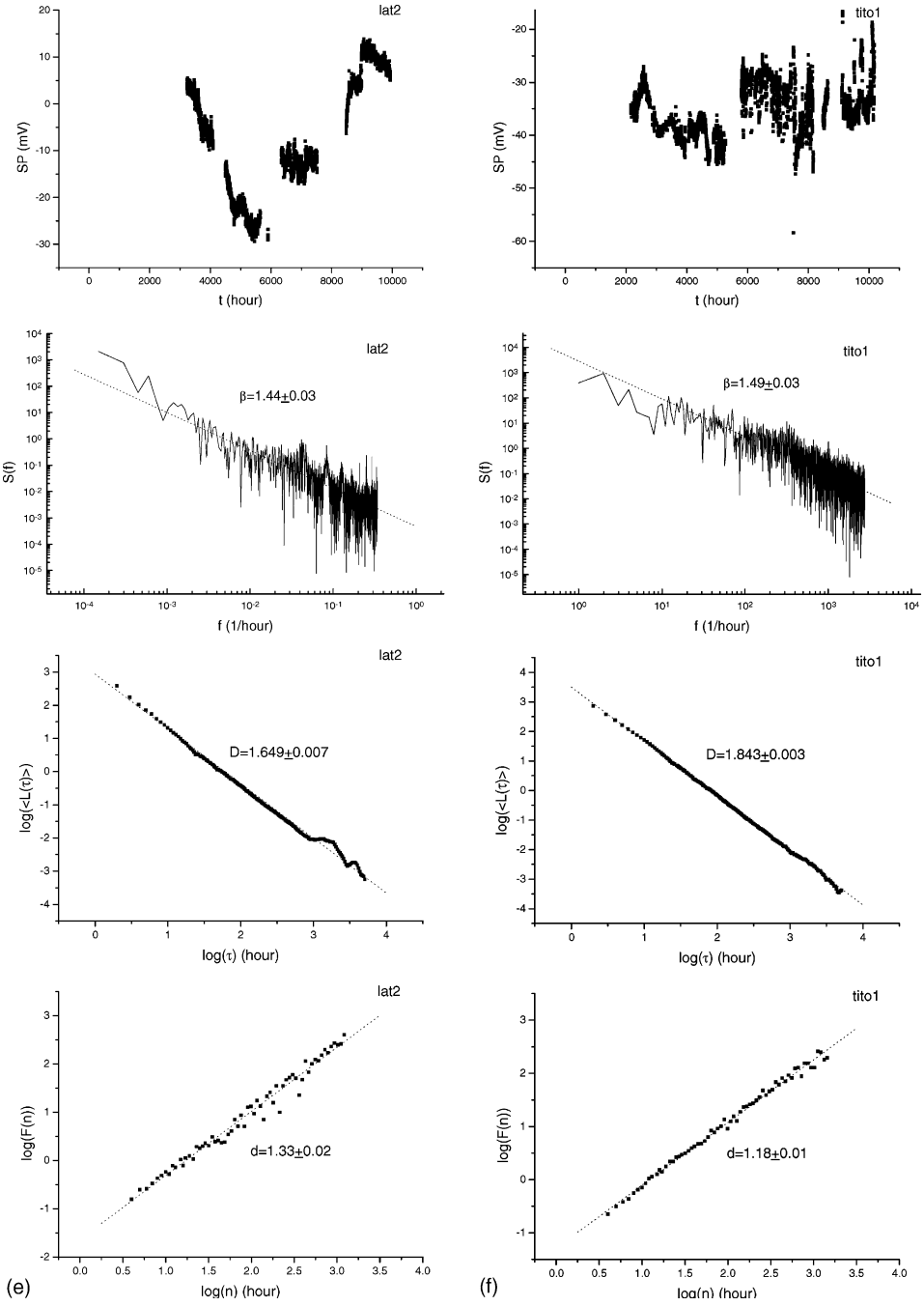

Fig. 2 (*continued*)

estimated, as the slope of the log–log plot of the length $L_{BK}(\tau)$ vs. the time interval τ. Then, using Berry's, the spectral exponent estimation can be estimated.

Another method which also gives a stable value of the fractal dimension has been presented by Higuchi [17,18]. A new time series is constructed from the given time series $X(i)$, $(i = 1, 2, \ldots, N)$,

$$X_\tau^m; X(m), X(m+\tau), X(m+2\tau), \ldots, X(m+[(N-m)/\tau]\tau); \quad (m = 1, \ldots \tau), \tag{4}$$

where [ ] denotes Gauss' notation. The length of the curve is defined as

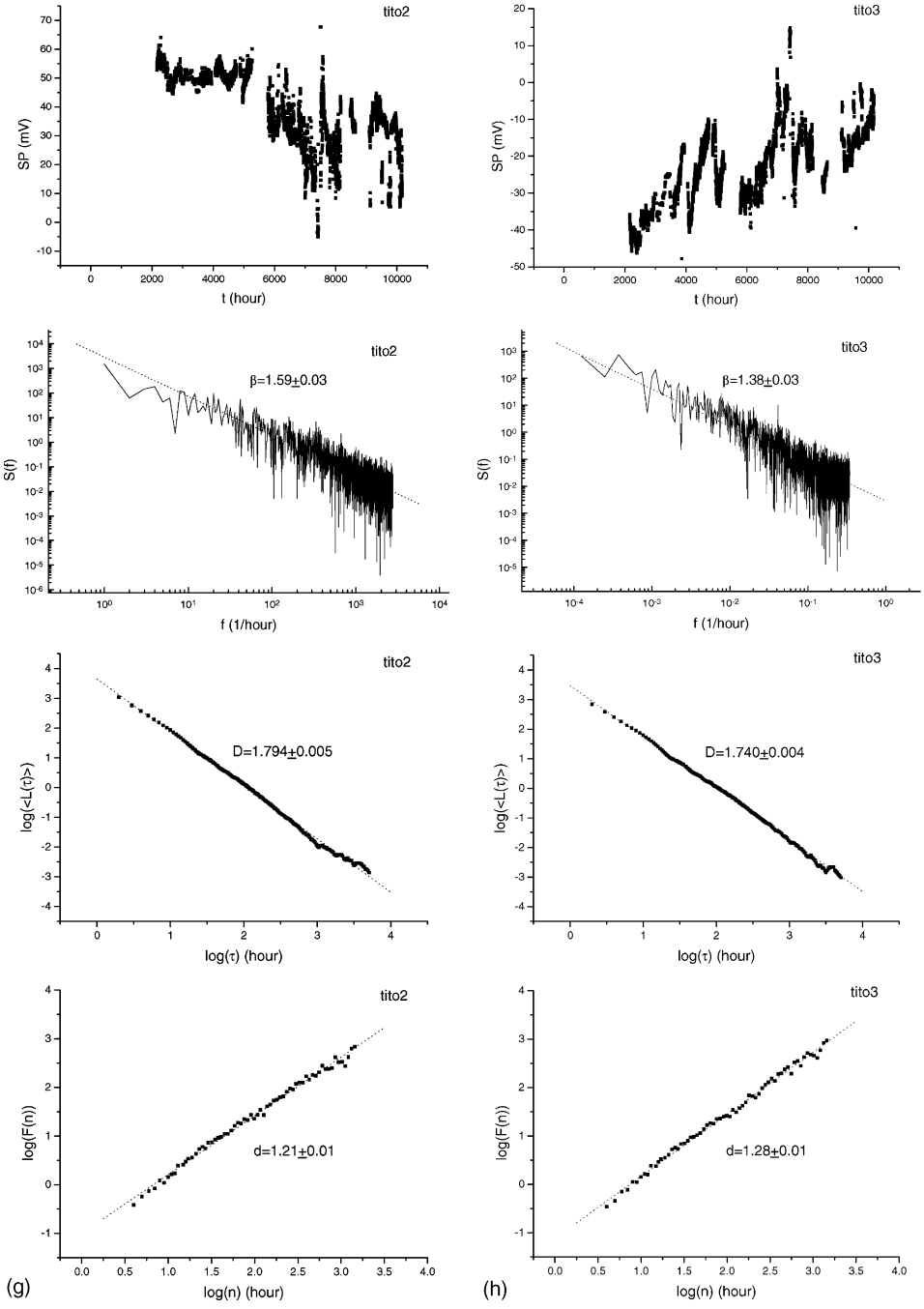

Fig. 2 (*continued*)

$$L_m(t) = \left\{ \left(\sum_{i=1}^{[(N-m)/\tau]} |X(m+i\tau) - X(m+(i-1)\tau| \right) \frac{N-1}{[(N-m)/\tau]\tau} \right\} \frac{1}{\tau}. \tag{5}$$

The average value $\langle L(\tau) \rangle$ over sets of $L_m(\tau)$ is defined as the length of the curve for the time interval τ. If $\langle L(\tau) \rangle \propto \tau^{-D}$, within the range $\tau_{\min} \leqslant \tau \leqslant \tau_{\max}$ then the curve is fractal with dimension D in this range. He examined the relationship between the fractal dimension D and the power-law index β, by calculating the fractal dimension of the simulated time

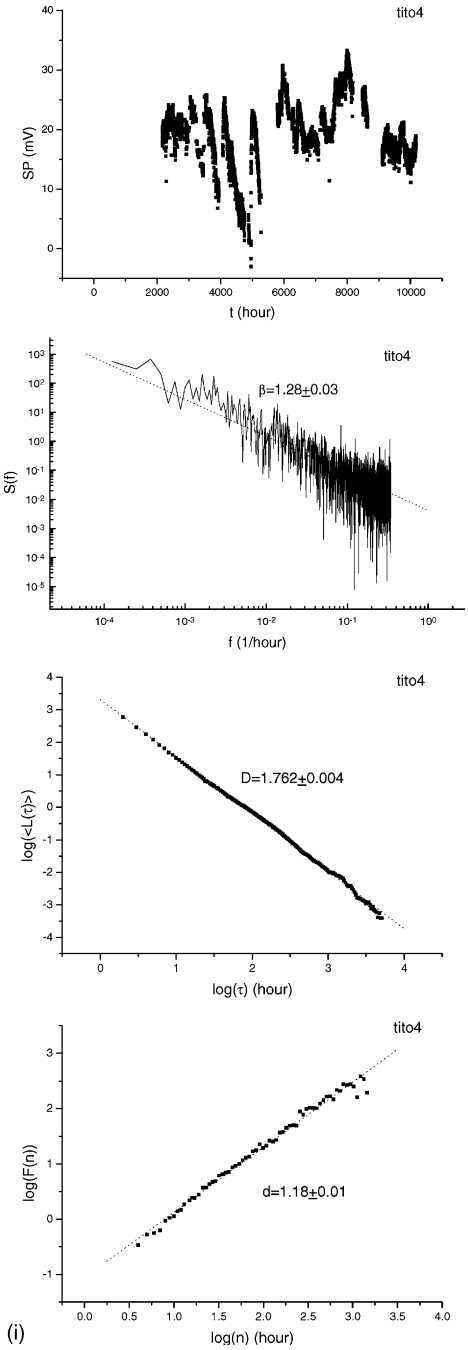

Fig. 2 (*continued*)

series which follows a single power-law spectrum density. Even in this case, the spectral exponent estimation could be carried out using Berry's expression.

Recently, the method of detrended fluctuation analysis (DFA) has been developed to reveal long-range correlation structures in observational time series. This method was proposed by Peng et al. [21], and it avoids spurious detection of correlations that are artifacts of nonstationarity, that often affects experimental data. Such trends have to be well distinguished from the intrinsic fluctuations of the system in order to find the correct scaling behaviour of the fluc-

tuations. Very often we do not know the reasons for underlying trends in collected data and we do not know the scales of underlying trends. DFA is a well-established method for determining the scaling behaviour of data in the presence of possible trends without knowing their origin and shape [22]. The methodology operates on the time series $x(i)$, where $i = 1, 2, \ldots, N$ and N is the length of the series. With x_{ave} we indicate the average value

$$x_{\text{ave}} = \frac{1}{N}\sum_{k=1}^{N} x(k). \tag{6}$$

The signal is first integrated

$$y(k) = \sum_{i=1}^{k}[x(i) - x_{\text{ave}}]. \tag{7}$$

Next, the integrated time series is divided into boxes of equal length n. In each box a least-squares line is fit to the data, representing the trend in that box. The y coordinate of the straight line segments is denoted by $y_n(k)$. Next we detrend the integrated time series $y(k)$ by subtracting the local trend $y_n(k)$ in each box. The root-mean-square fluctuation of this integrated and detrended time series is calculated by

$$F(n) = \sqrt{\frac{1}{N}\sum_{k=1}^{N}[y(k) - y_n(k)]^2}. \tag{8}$$

Repeating this calculation over all box sizes n, we obtain a relationship between $F(n)$, that represents the average fluctuation as a function of box size, and the box size n. If $F(n)$ behaves as a power-law function of n, data present scaling:

$$F(n) \propto n^d. \tag{9}$$

Under these conditions the fluctuations can be described by the scaling coefficient d, representing the slope of the line fitting $\log F(n)$ to $\log n$. The values of exponent d may represent a range of processes. For example $d = 0.5$ means that the signal samples are uncorrelated or short-range-correlated. An exponent $d \neq 0.5$ in a certain range of scales n suggests the existence of long-range correlations. If $d = 1.0$ the temporal fluctuations are of flicker-noise type; if $d = 1.5$ the temporal fluctuations are of Brownian type. The DFA scaling exponent d and the spectral exponent β are related to each other as described in [23,24] by the following equation:

$$d = \frac{1+\beta}{2}. \tag{10}$$

3.2. Multifractal formalism and parameters

The concept of multifractal object has been developed by Mandelbrot [25] to investigate several features in the intermittency of turbulence [26]. Many authors have applied the multifractality to several fields of the scientific research.

The multifractal formalism is based on the definition of the so-called partition function $Z(q, \varepsilon)$,

$$Z(q, \varepsilon) = \sum_{i=1}^{N_{\text{boxes}}(\varepsilon)} \mu_i(\varepsilon). \tag{11}$$

The quantity $\mu_i(\varepsilon)$ is a measure and it depends on ε, the size or scale of the boxes used to cover the sample. The boxes are labeled by the index i and $N_{\text{boxes}}(\varepsilon)$ indicates the number of boxes of size ε needed to cover the sample. The exponent q is a real parameter, giving the order of the moment of the measure. The choice of the functional form of the measure $\mu_i(\varepsilon)$ is arbitrary, provided that the most restrictive condition $\mu_i(\varepsilon) \geqslant 0$ is satisfied.

The parameter q can be considered as a powerful microscope, able to enhance the smallest differences of two very similar maps [27]. Furthermore, q represents a selective parameter: high values of q enhance boxes with relatively high values for $\mu_i(\varepsilon)$; while low values of q favor boxes with relatively low values of $\mu_i(\varepsilon)$. The box size ε can be considered as a filter, so that big values of the size is equivalent to apply a large scale filter to the map. Changing the size ε, one explores the sample at different scales. Therefore, the partition function $Z(q, \varepsilon)$ furnishes information at different scales and moments.

The generalized dimension are defined by the following equation

$$D(q) = \lim_{\varepsilon \to 0} \frac{1}{q-1}\frac{\ln Z(q, \varepsilon)}{\ln \varepsilon}. \tag{12}$$

$D(0)$ is the capacity dimension; $D(1)$ is the information dimension, and $D(2)$ is the correlation dimension. An object is called monofractal if $D(q)$ is constant for all values of q, otherwise is called multifractal. In most practical applications the limit in Eq. (12) cannot be calculated, because we do not have information at small scales, or because below a minimum physical length no scaling can exist at all [27]. Generally, a scaling region is found, where a power-law can be fitted to the partition function, which in that scaling range behaves as

$$Z(q,\varepsilon) \propto \varepsilon^{\tau(q)}. \tag{13}$$

The slope $\tau(q)$ is related to the generalized dimension by the following equation:

$$\tau(q) = (q-1)D(q). \tag{14}$$

An usual measure in characterizing multifractals is given by the singularity spectrum or Legendre spectrum $f(\alpha)$, that is defined as follows. If for a certain box j the measure scales as

$$\mu_j(\varepsilon) \propto \varepsilon^{\alpha_j} \tag{15}$$

the exponent α, which depends upon the box j, is called Hölder exponent. If all boxes have the same scaling with the same exponent α, the sample is monofractal. The multifractal is given if different boxes scale with different exponents α, corresponding to different strength of the measure. Denoting as S_α the subset formed by the boxes with the same value of α, and indicating as $N_\alpha(\varepsilon)$ the cardinality of S_α, for a multifractal the following relation holds:

$$N_\alpha(\varepsilon) \propto \varepsilon^{-f(\alpha)}. \tag{16}$$

By means of the Legendre transform the quantities α and $f(\alpha)$ can be related with q and $\tau(q)$:

$$\alpha(q) = \frac{\mathrm{d}\tau(q)}{\mathrm{d}q}, \tag{17}$$

$$f(\alpha) = q\alpha(q) - \tau(q). \tag{18}$$

The curve $f(\alpha)$ is a single-humped function for a multifractal, while reduces to a point for a monofractal.

In order to quantitatively recognize possible differences in Legendre spectra stemming from different signals, it is possible to fit, by a least square method, the spectra to a quadratic function around the position of their maxima at α_0 [28]:

$$f(\alpha) = A(\alpha-\alpha_0)^2 + B(\alpha-\alpha_0) + C. \tag{19}$$

Parameter B measures the asymmetry of the curve, which is zero for symmetric shapes, positive or negative for left-skewed or right-skewed shapes, respectively.

Another parameter is the width of the spectrum, that estimates the range of α where $f(\alpha) > 0$, obtained extrapolating the fitted curve to zero; thus the width is defined as

$$W = \alpha_{\max} - \alpha_{\min}, \tag{20}$$

where $f(\alpha_{\max}) = f(\alpha_{\min}) = 0$.

These three parameters serve to describe the "complexity" of the signal. If α_0 is low, the signal is correlated and the underlying process "loses fine structure", becoming more regular in appearance [28]. The width W measures the length of the range of fractal exponents in the signal; therefore, the wider the range, the "richer" the signal in structure. The asymmetry parameter B informs about the dominance of low or high fractal exponents respect to the other. A right-skewed spectrum denotes relatively strongly weighted high fractal exponents, corresponding to fine structures, and low ones (more smooth-looking) for left-skewed spectra.

4. Results

We performed monofractal and multifractal analysis on nine hourly geoelectrical time series, measured by four stations located in different sites in southern Italy. The time series cover the period from January 2001 to February 2002. Fig. 2 shows the time variation, the Lomb spectrum, the Higuchi analysis and the DFA results for each signal.

The Lomb spectra, that estimate the power spectral density for unevenly sampled signal, are not flat; this indicates that self-potential signals are not realizations of purely random variables. We can clearly observe a common decreasing power-law behaviour, characterized by different scaling exponents, estimated by the slopes of the line that fits by a least

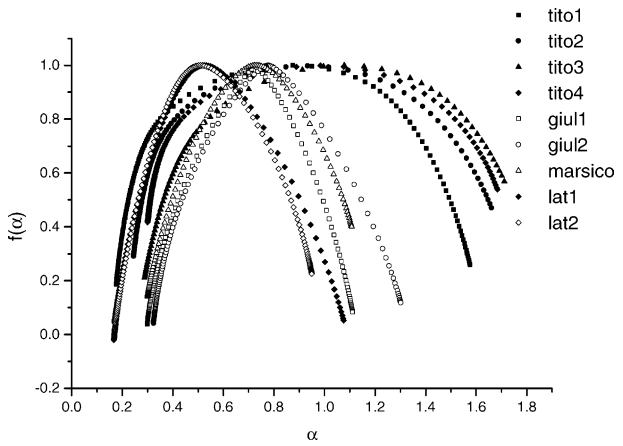

Fig. 3. Legendre spectra of the signals measured in southern Italy. All the spectra evidence the single-humped shape, typical of multifractal signals. The curve display clear differences in maximum, symmetry and width.

square method the spectrum, plotted in log–log scales: the spectral exponents α range from $\sim$1.3 to 1.9. The most of the time series evidence spectral spikes at cycles of 12 and 24 hours, superimposed on the power-law behaviour of the spectrum. The Higuchi analysis reveals scaling behaviours with different values of the scaling exponent D ranging from approximately 1.3 and 1.8. Scaling behaviour is also shown by the results of the DFA applied to the analyzed signals. The value of the scaling exponent d varies from approximately 1.2 and 1.4. The estimates of d give spectral exponents slightly different from the sepctral exponents calculated by means of the Lomb Periodogram. Stanley et al. [29] argue that there is a theoretical support for the hypothesis that DFA produces less noisy plots. They link DFA to a double summation of the series autocorrelation function, while the power spectrum is derived from a Fourier transformation of the autocorrelation. The double summation acts effectively as a noise filter, providing more accurate estimates.

We performed the multifractal analysis, calculating the Legendre spectra by means of the software FRACLAB, developed at INRIA and available at the internet site http://www-rocq.inria.fr. Since the data present gaps, we analyzed for each signal the longest segment without data missings. The length of each segment is about 10^3, thus permitting to obtain reliable estimates of the singularity spectrum and multifractal parameters. The results are shown in Fig. 3. All the spectra present the typical single-humped shape, that characterizes multifractal signals. The differences among the spectra are very clear. Thus, after the determination of the maxima α_0, we fitted each spectrum by Eq. (19), thus estimating the asymmetry B and the width W. The results are summarized in Fig. 4. The time series lat1 and lat2, measured in station Laterza located in an aseismic area, present the lowest value for the maximum α_0 (Fig. 4a), indicating a more regular process governing the time variability of such signals, that seem to characterized by more "coarse" structures. The smooth-looking behaviour displayed by lat1 and lat2 is recognized also in the Fig. 4b, where the asymmetry B assumes the highest positive value for such signals. The signals measured by station Tito (tito1, tito2, tito3 and tito4) appear more complex than the rest, because they present the highest maximum α_0 values, the highest width W values and relatively low value for the asymmetry B. We have plotted the multifractal measures shown in a 3-D diagram, whose axes are the maximum α_0, the asymmetry B and the width W (Fig. 5): the signals lat1 and lat2 seem to be well separated from the rest. Projecting the points on the planes (α_0, B), (α_0, W) and (B, W) (Fig. 6), we find a clear discrimination between signals measured in a seismic area (giul1, giul2, tito1, tito2, tito3, tito4 and marsico) and signals measured in an aseismic area (lat1 and lat2).

5. Discussion

The geophysical phenomenon underlying the geoelectrical variations is complex and the physical laws that govern the process are not completely known. The use of monofractal and multifractal methods in investigating the temporal fluctuations of geoelectrical signals can lead to a better understanding of such complexity.

Recently, the complex dynamics of extended systems have been analyzed. These systems are very common in nature and a typical effect in the time domain is known as $1/f$ noise or flicker-noise, so the power spectra of these processes exhibit a linear behaviour on a log–log scale.

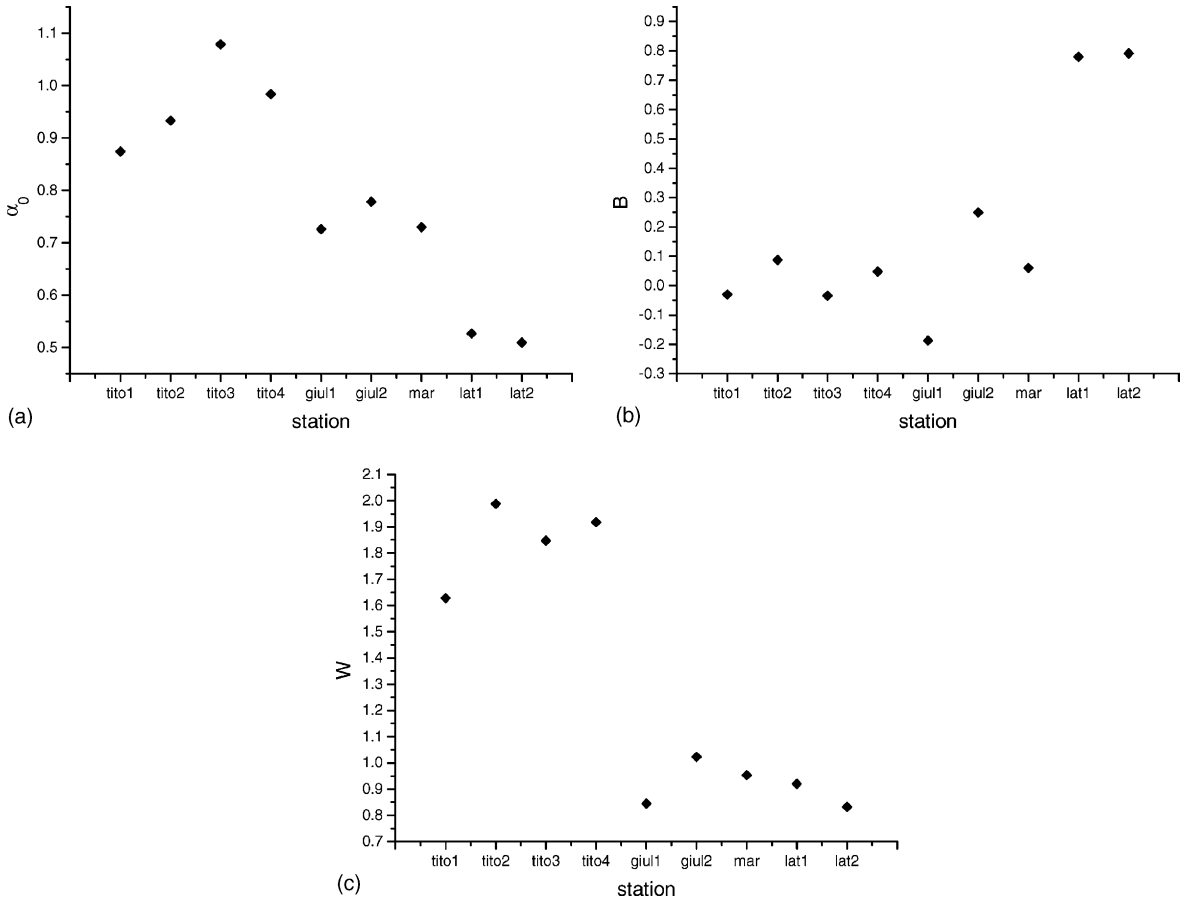

Fig. 4. Variation with the station of the multifractal parameters: maximum α_0 (a), asymmetry B (b) and width W (c). lat1 and lat2 seem to be less complex than the others, while tito1–4 signals appear more complex than the rest.

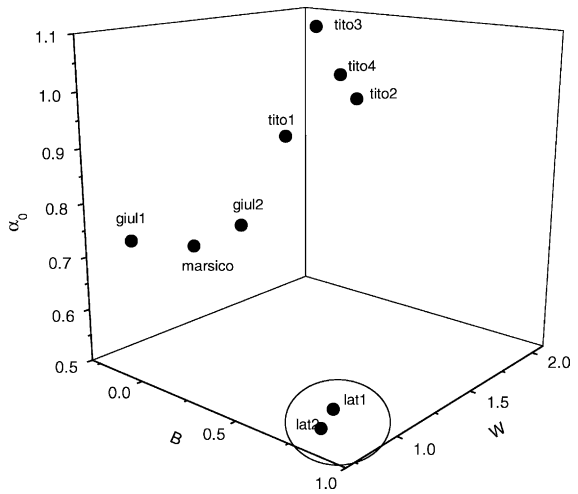

Fig. 5. 3-D plot of the multifractal parameters: the series lat1 and lat2, measured in aseismic area, seem to be well separated from the remaining time series.

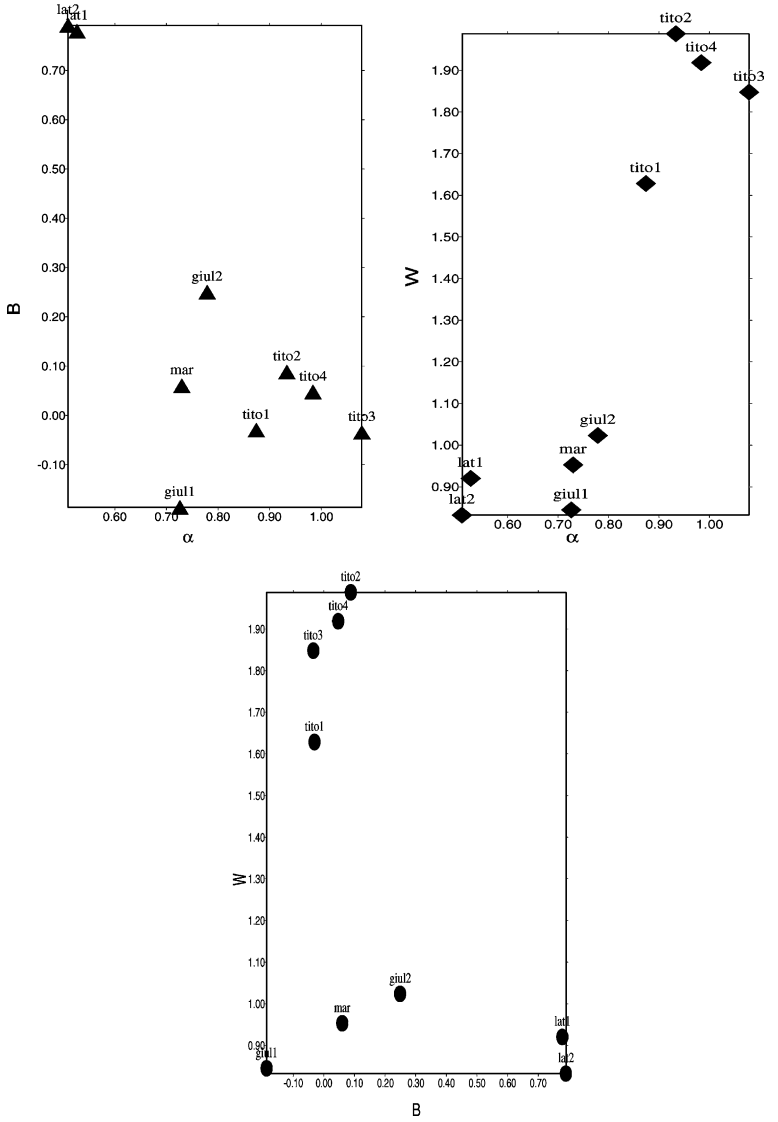

Fig. 6. Projections of the 3-D plot of Fig. 5 onto the planes (α_0, B), (α_0, W) and (B, W). A clear evidence of the discrimination between geoelectrical signals recorded in seismic and aseismic areas is shown.

Today studies on the dynamics of these extended systems are carried out in many different research fields and the theory of the self-organized critical state (SOC) provides a connection between nonlinear dynamics, self-similarity and $1/f$ noise. In particular many authors (e.g. [30–32]) used this theory to investigate and simulate the physical process responsible for earthquakes. Scaling laws in earthquake sequences are related to the complexity of the crust. The lithosphere presents a hierarchy of volumes, or blocks, which move in relation to each other and are divided into smaller blocks, like shields or mountain chains. The stress field determines continental collisions situations and as consequence the accumulated strain energy is radiated as seismic waves [33].

According to the hypothesis of Turcotte [34], the tectonic of the earth and all the unexplained correlations of geophysical and geoelectrical fields over the earth surface can be considered as a sequence of instability episodes, and the presence of scaling laws in the statistics describing the fluctuations of these signals can lead to a collective statistical phenomenon in agreement with the SOC interpretation of the earthquake process.

The evolution of the earth's crust toward the self-organized critical state takes place not only in a seismological sense, as formation of the block-spring fractal structure in the fault zone, but also in the electromagnetic sense as a

probable formation of the fractal conductor-dielectric structure. Such a system consisted of porous medium could develop, in one way, as decomposition of elements on smaller scales, or in another way, as composition of the larger scale structure. Both of those processes could cause the scaling characteristics of geoelectrical signals and seismogenic integral emissions from crack microcurrents [35].

By means of fractal tools we extracted quantitative information about the complexity, involving the time dynamics of the geoelectrical signals recorded in southern Italy, one of the most seismically active region of the Mediterranean area. The monofractal analyses have shown the presence of scaling behaviours in all the signals measured, this implying the existence of correlated time structures.

The determination of the multifractal parameters has been performed by means of the calculation of the Legendre spectrum. We derived three parameters, the maximum α_0 of the spectrum, the asymmetry B and the width W of the curve. The time series lat1 and lat2, recorded in an aseismic site, are characterized by low maximum α_0, high positive asymmetry B and low width W. These features qualify these time series as less complex than the others (tito1–4, giul1–2 and Marsico), which have been measured in seismic sites. Therefore, this set of multifractal parameters seem to well discriminate signals measured in seismic from signal recorded in aseismic sites.

6. Conclusions

We have shown that the time dynamics of the geoelectrical time series measured in a seismic active area of southern Italy are not realizations of a purely random stochastic process. The Lomb power spectra have the power-law form typical of colored-noise with the spectral exponent measuring the degree of correlations in the signals, this indicating the presence of memory effects in the geophysical system generating geoelectrical signals. The Higuchi analysis has revealed that geoelectrical signals presents typical features of fractal curves with scaling exponents D consistent with the spectral indices. The DFA has shown the presence of long-range correlations in the data. The multifractal formalism applied to the analyzed time series, aimed to the determination of a set of multifractal parameters, has revealed its power of discrimination between signals measured in seismic sites from signal recorded in a seismic sites.

References

[1] Park SK. Monitoring resistivity change in Parkfield, California: 1988–1995. J Geophys Res 1997;102:24545–59.
[2] Johnston MJS. Review of electric and magnetic fields accompanying seismic and volcanic activity. Survey Geophys 1997;18:441–75.
[3] Scholz CH. In: The mechanics of earthquakes and faulting. Cambridge University Press; 1990. p. 439.
[4] Raleigh B, Bennet G, Craig H, Hanks T, Molnar P, Nur A, et al. Prediction of the Haicheng earthquake. EOS Trans Am Geophys Union 1977:236–72.
[5] Varotsos P, Alexopoulos K, Lazaridou M. Latest aspects of earthquake prediction in Greece based on seismic electric signals. Tectonophysics 1993;224:1–39.
[6] Burton PW. Electrical earthquake prediction. Nature 1985;315:315–7.
[7] Mulargia F, Gasperini P. Evaluating the statistical validity beyond chance of earthquake precursors. Geophys J Int 1992;111:32–44.
[8] Hayakawa M, editor. Atmospheric and ionospheric electromagnetic phenomena associated with earthquakes. Tokyo: Terra Sci. Pub. Co; 1999. p. 997.
[9] Hayakawa M, Fujinawa Y, editors. Electromagnetic phenomena related to earthquake prediction. Tokyo: Terra Sci. Pub. Co; 1994. p. 667.
[10] Cuomo V, Lapenna V, Macchiato M, Serio C, Telesca L. Linear and non linear dynamics in electrical precursory time series: implications with earthquake prediction. Tectonophysics 1998;287:279–98.
[11] Di Maio R, Patella D. Basic theory of electrokinetic effects associated with earthquakes. Boll Geofis Teor Appl 1991;33:130–41.
[12] Patella D, Tramacere A, Di Maio R. Modelling earth current precursors in earthquake prediction. Anal Geofis 1997;40:495–517.
[13] Cassano E, Fichera R, Arisi Rota F. Aeromagnetic survey of Italy: a few interpretative results. Technical Report, AGIP-DES-MSEG, 1986. p. 13.
[14] Balderer W, Martinelli G. Geochemistry of groundwaters and gases occurring in the November 23, 1980 earthquake area. Environ Geochem 1994;16(Suppl):147–64.
[15] Doglioni C, Harabaglia P, Martinelli G, Mongelli F, Zito G. A geodynamic model of the Southern Apennines accretionary prism. Terra Nova 1996;8:540–7.
[16] Lomb NR. Least-squares frequency analysis of unequally spaced data. Astrophys Space Sci 1976;39:447–62.
[17] Higuchi T. Approach to an irregular time series on the basis of the fractal theory. Physica D 1988;31:277–83.
[18] Higuchi T. Relationship between the fractal dimension and the power-law index for a time series: a numerical investigation. Physica D 1990;46:254–64.

[19] Burlaga LF, Klein LW. Fractal structure of the interplanetary magnetic field. J Geophys Res 1986;91:347–51.
[20] Berry MV. Diffractals. J Phys A Math Gentile 1979;12:781–92.
[21] Peng C-K, Havlin S, Stanley HE, Goldberger AL. Quantification of scaling exponents and crossover phenomena in nonstationary heartbeat time series. Chaos, Solitons & Fractals 1995;5:82–7.
[22] Kantelhardt JW, Koscienly-Bunde E, Rego HHA, Havlin S, Bunde A. Detecting long-range correlations with detrended fluctuation analysis. Physica A 2001;295:441–54.
[23] Buldyrev SV, Goldberger AL, Havlin S, Peng C-K, Stanley HE. Fractals in biology and medicine. In: Bunde A, Havlin S, editors. Fractals in Science. Springer-Verlag; 1994.
[24] Havlin S, Selinger R, Schwartz M, Stanley HE, Bunde A. Random multiplicative processes and transport in structures with correlated spatial disorder. Phys Rev Lett 1988;61:1438–41.
[25] Mandelbrot BB. Intermittent turbulence in self-similar cascades: divergence of high moments and dimensions of the carrier. J Fluid Mech 1974;62:331–58.
[26] Meneveau C, Sreenivasan KR. The multifractal nature of turbulent energy dissipation. J Fluid Mech 1991;224:429–84.
[27] Diego JM, Martinez-Gonzales E, Sanz JL, Mollerach S, Mart VJ. Partition function based analysis of cosmic microwave background maps. Mon Not R Astron Soc 1999;306:427–36.
[28] Shimizu Y, Thurner S, Ehrenberger K. Multifractal spectra as a measure of complexity in human posture. Fractals 2002;10:103–16.
[29] Stanley HE, Afanasyev V, Amaral LAN, Buldyrev SV, Goldberger AL, Havlin S, et al. Anomalous fluctuations in the dynamics of complex systems: from DNA and physiology to econophysics. Physica A 1996;224:302–21.
[30] Sornette A, Sornette D. Earthquake rupture as a critical point consequences for telluric precursors. Tectonophysics 1990;179:327–34.
[31] Crisanti A, Jensen MH, Vulpiani A, Paladin G. Strongly intermittent chaos and scaling in an earthquake model. Phys Rev Lett 1992;46:7363–6.
[32] Grassberger P. Efficient large-scale simulation of a uniformly driven system. Phys Rev E 1994;49:2436–43.
[33] Keilis-Borok VI. The lithosphere of the earth as a nonlinear system with implications for earthquake prediction. Rev Geophys 1990;28:19–34.
[34] Turcotte DL. In: Fractals and chaos in geology and geophysics. Cambridge: Cambridge University Press; 1992. p. 221.
[35] Hayakawa M, Ito T, Smirnova N. Fractal analysis of ULF geomagnetic data associated with the Guam earthquake on August 8 1993. Geophys Res Lett 1999;26:2797–800.